

PAPER • OPEN ACCESS

## Synthesis of solvent-free conductive and flexible cellulose–carbon nanohorn sheets and their application as a water vapor sensor

To cite this article: Karthik Paneer Selvam *et al* 2020 *Mater. Res. Express* 7 056402

View the [article online](#) for updates and enhancements.



**IOP | ebooks™**

Bringing together innovative digital publishing with leading authors from the global scientific community.




Start exploring the collection—download the first chapter of every title for free.



## PAPER

## Synthesis of solvent-free conductive and flexible cellulose–carbon nanohorn sheets and their application as a water vapor sensor

## OPEN ACCESS

RECEIVED  
12 January 2020REVISED  
2 April 2020ACCEPTED FOR PUBLICATION  
16 April 2020PUBLISHED  
4 May 2020Karthik Paneer Selvam , Tomohiro Nakagawa, Tatsuki Marui, Hiroataka Inoue , Takeshi Nishikawa and Yasuhiko Hayashi 

Graduate School of Natural Science and Technology, Okayama University, Okayama, 700-8530, Japan

E-mail: [hayashi.yasuhiko@okayama-u.ac.jp](mailto:hayashi.yasuhiko@okayama-u.ac.jp)

Keywords: carbon nanohorns, cellulose, conductive sheets, vapor sensor

Original content from this work may be used under the terms of the [Creative Commons Attribution 4.0 licence](https://creativecommons.org/licenses/by/4.0/).

Any further distribution of this work must maintain attribution to the author(s) and the title of the work, journal citation and DOI.



## Abstract

Carbon nanohorns (CNHs) are mixed with cellulose to make freestanding thin-film conductive sheets. CNHs, at different ratios (5, 10, 25, 50 wt%), form composites with cellulose (hydroxyethylcellulose). Freestanding cellulose–carbon nanohorn (CCN) sheets were fabricated using a 100  $\mu\text{m}$ -thick metal bar coater. Surfactants or any other chemical treatments to tailor the surface properties of CNHs were avoided to obtain composite sheets from pristine CNHs and cellulose. Utilizing the hygroscopic property of hydroxyethylcellulose and the electrical conductivity of CNHs paved a path to perform this experiment. The synthesis technique is simple, and the fabrication and drying of the sheets were effortless. As the loading concentration of CNH increased, the resistance, flexibility, and strength of the CCN composite sheets decreased. The maximum loading concentration possible to obtain a freestanding CCN sheet is 50 wt%. The resistance of the maximum loading concentration of CNH was 53 k $\Omega$ . The response of the CCN sheets to water vapor was 4 s and recover time was 13 s, and it is feasible to obtain a response for different concentrations of water vapor. High-resolution transmission electron microscopy, scanning electron microscopy, Fourier transform infrared spectroscopy, Raman spectroscopy, resistance measurement, tensile strength measurement, and thermogravimetric analysis were used to investigate the mechanical, morphological, electrical, and chemical properties of the CCN sheets.

## 1. Introduction

Sustainable and biodegradable materials are always widely accepted and preferred in materials research. Cellulose is an inexhaustible material with excellent prospects for applications in various areas of science [1]. Cellulose is an abundantly available natural polymer [2] that is used on an industrial scale in many applications, specifically in drug delivery [3] and, bio-sensing [4]. Depending on the occurrence cellulose is classified broadly into cellulose I, cellulose II (regenerated cellulose), and lignocellulose [5]. Cellulose research in materials science has been ongoing since it began, in 2002, with the dissolution of cellulose using ionic liquids carried out by Swatloski *et al* [6].

Carbon nanohorns (CNH) are an allotrope of carbon [7] with properties similar to carbon nanotubes (CNTs) and are an avowed material for many advanced applications in materials science. Generally, CNHs are produced by the arc discharge method, which yields high purity with tubule lengths of 30–50 nm and an angle length of 20° [8–10]. CNHs have the unique properties of high specific areas and large pore volumes. Conical structure of the CNHs may assist in obtaining high dispersion and the formation of a composite with cellulose. Unlike carbon nanotubes, which require acid treatments or surfactants to disperse [11], CNHs are likely to disperse well in solvents. Hence this distinct property can aid in the interaction between cellulose and CNHs.

Recently, active materials for sensing applications have been gathering tremendous attention. Carbon nanotubes are quite prominent in the nanomaterials that are predominantly considered [12]. Sensor manufacturing is always seeking devices that are low-cost, highly efficient, and easy to synthesize and procure.

Sensors based on carbon nanotubes are mostly employed by altering the CNTs electrical conductivity of the CNTs with a variety of gases, such as  $\text{NO}_2$  [13], but need a temperature of  $200^\circ\text{C}$  to work [14]. Some metal decorated CNTs are also found to have sensing applications [15]. Relative humidity sensors employing multi-walled carbon nanotubes (MWCNTs) are reported with a sensitivity range from 11% to 98% for untreated MWCNTs [16]. Suspended functionalized single-walled carbon nanotubes (SWCNTs) were also synthesized with low-hysteresis and fast response with a response time of 12 s, and a recover time of 47 s [17]. However, these reports doesnot include cellulose in the active part of the sensor. CNHs are electrically conductive and chemically inert nanomaterials, hence synthesizing composite materials using CNHs necessitates a novel approach.

To obtain an ideal conductive sheet, a homogeneous mixture of CNH and cellulose is required to improve the properties of the sheets. An ideal conductive sheet should possess good conductivity, strength, and flexibility. It is well known that chemical modifications of carbon nanomaterials by surfactants or acid treatments can improve the dispersion functionality, but they can affect other properties [18]. If a CNT or CNH has a carboxyl functional group, it binds strongly with cellulose. The present work deals with synthesizing cellulose carbon nanohorn (CCN) sheets and measuring the pristine properties of cellulose and CNH composites when drawn as sheets. Parameters such as electrical conductivity and tensile strength are mainly focused on in relation to other measurements such as a change in conductivity in dry and wet conditions where a possibility of sensor application can be determined. This measurement would enable us to understand and calibrate the properties of modified cellulose and CNHs, as well as other dopants in the vicinity of the composite. According to our literature survey, this report is the first of its kind in exploring the composite of CNHs and cellulose sheets and their conductivity in different loading concentrations. CNTs have long and tangled structures that, when dispersed, require cellulose to hold each CNT in the matrix together. CNHs, on the other hand, have CNH aggregates as the default arrangement, hence allowing the cellulose to have a composite on the external layer of the CNH aggregate, which helps the CNH aggregates to preserve their pristine properties, as seen in the high-resolution transmission electron microscopy images.

## 2. Method

As-received bud-like structured CNHs of over 90% purity and hydroxyethylcellulose (HEC) were used as precursors to perform this experiment. Different ratios of CNHs (5, 10, 25, 50 wt%) were dispersed in 10 mL of distilled water separately and agitated. Ethanol (5 ml) was added to each solution and sonicated in a water bath sonicator for one hour to obtain a homogeneous dispersion of CNHs. Cellulose (200 mg) was dissolved in 5 ml of distilled water and sonicated for an hour, resulting in a highly viscous, colorless solution. Each solution of CNHs is mixed with the cellulose solution and sonicated for 1 h. The CCN solution was then placed on a hot plate with stirring for 6 h at  $150^\circ\text{C}$ . Excess distilled water was removed by heating and stirring, resulting in a thick black paste of CCN composite. The total volume was reduced to about 95 wt %. This paste of CCN composite was then fabricated as sheets on a clean glass plate by a  $100\ \mu\text{m}$  metal bar applicator to obtain uniform thickness. After drawing sheets on the glass plate, the sheets were dried. Uniform-sized sheets were cut and peeled off the glass plate to make freestanding CCN sheets that were analyzed for its properties. The graphical illustration of the freestanding CCN composite sheets synthesis and the testing of its conductivity is shown below in figure 1.

### 2.1. Characterization

A high-resolution transmission electron microscope (HR-TEM; JEOL JEM-2100F) operating at 200 kV was used for morphological characterization. A scanning electron Microscope (SEM, JSM 6060LA, JEOL) was used to observe the morphology of the CCN sheets. A laser Raman spectrometer (JASCO NRS-5100 Nps) was used to investigate the D and G bands of CNH cellulose composites. Functional groups in the CNH cellulose composite are identified using a Fourier transform infrared spectrometer (JASCO FTIR 4100). Thermogravimetric analysis (SHIMADZU DTG-60) was performed to investigate the thermal stability of CCN sheets. Resistance measurements (ADCMT 6423 DC Voltage Current Source/Monitor) were performed on CCN sheets of different loading concentrations. Tensile strength (SHIMADZU AGS-X 5 N) was measured to find the intrinsic strength of the different CCN sheets.

## 3. Results and discussion

When compared to the composite of cellulose and SWCNTs, due to the presence of van der Waals forces, SWCNTs have a nonreactive surface and strong aggregation, resulting in a noneffective composite formation with cellulose [6]. This effect is reduced in the case of CNHs due to the presence of aggregates with conical tips

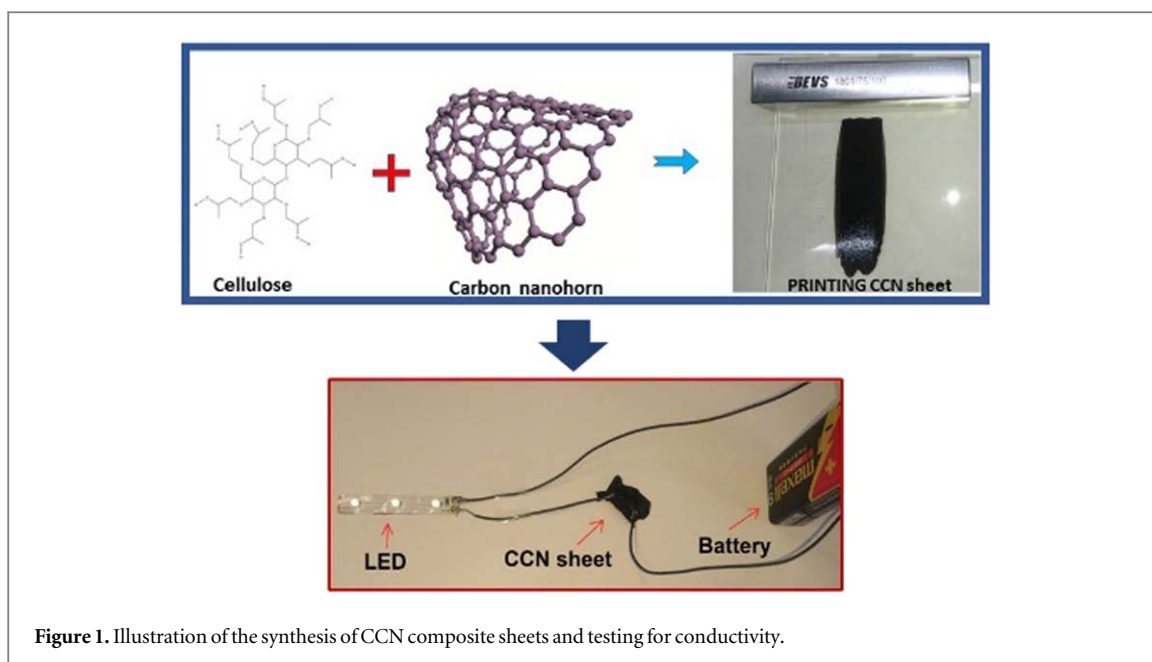


**Figure 1.** Illustration of the synthesis of CCN composite sheets and testing for conductivity.

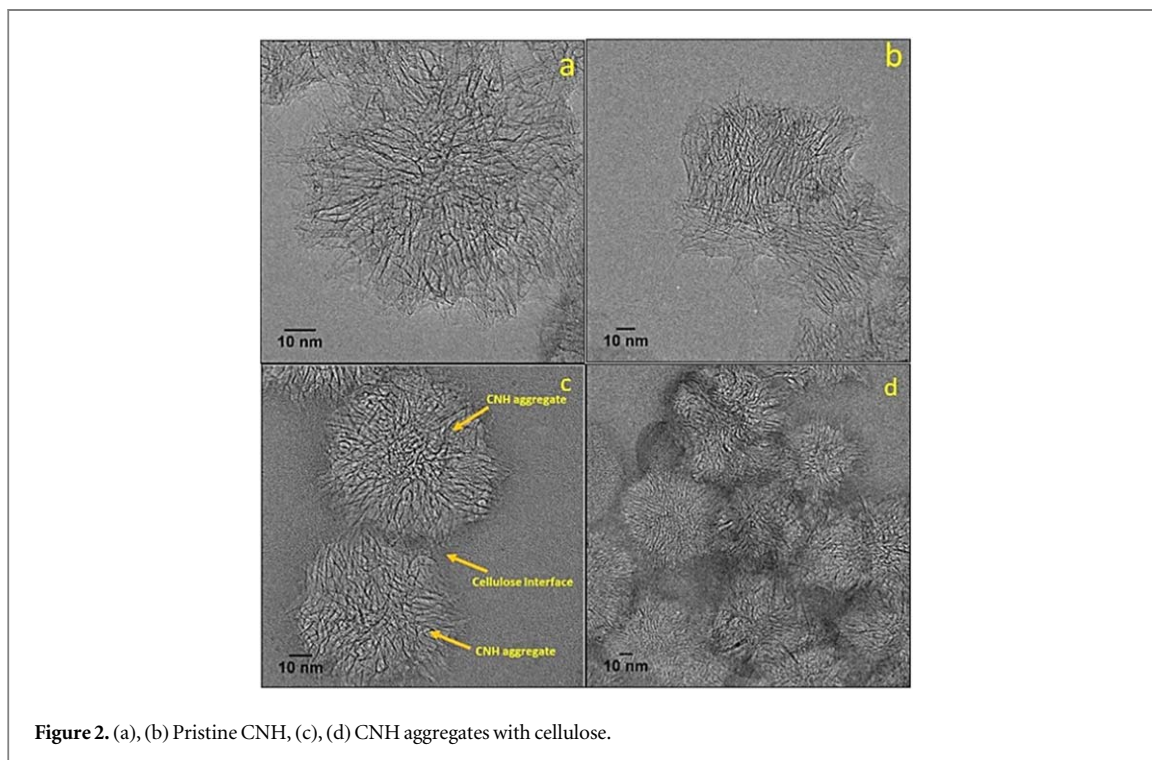


**Figure 2.** (a), (b) Pristine CNH, (c), (d) CNH aggregates with cellulose.

outside that help in active composite formation with cellulose. TEM images (figures 2(a) and (b)) show the pristine CNHs form aggregates with the conical tips protruding outwards of the aggregates. Figures 2(c) and (d), show the CCN composites that formed at the edges of the aggregates of the CNHs, hence forming a layer of cellulose encapsulation around the aggregates, also binding the neighboring CNH aggregate by acting as a bridge connecting the two aggregates of CNHs. This is observed for all the CNH aggregates, which indicates that hydroxyethylcellulose forms an excellent interface between the CNH aggregates due to the long polymer chains present in cellulose. This helps in obtaining the shapes of thin films. Also, a minimum amount of cellulose is adequate to encourage the formation of CCN composite sheets. Hence a conductive path is established in the random network of interconnected CNH aggregates. The electrical resistance ( $R$ ) was measured by two electrodes of nickel held by alligator pins and placed on the CCN sheet at a separation of 5 mm. The resistance measurement for each sample was performed four times to average the resistance value a typical plot of  $I-V$  is shown in figure 3. The resistance decreased with an increase in the concentration of CNH loading, as seen in table 1, and similarly, the tensile strength decreased with an increase in the CNH loading concentration.

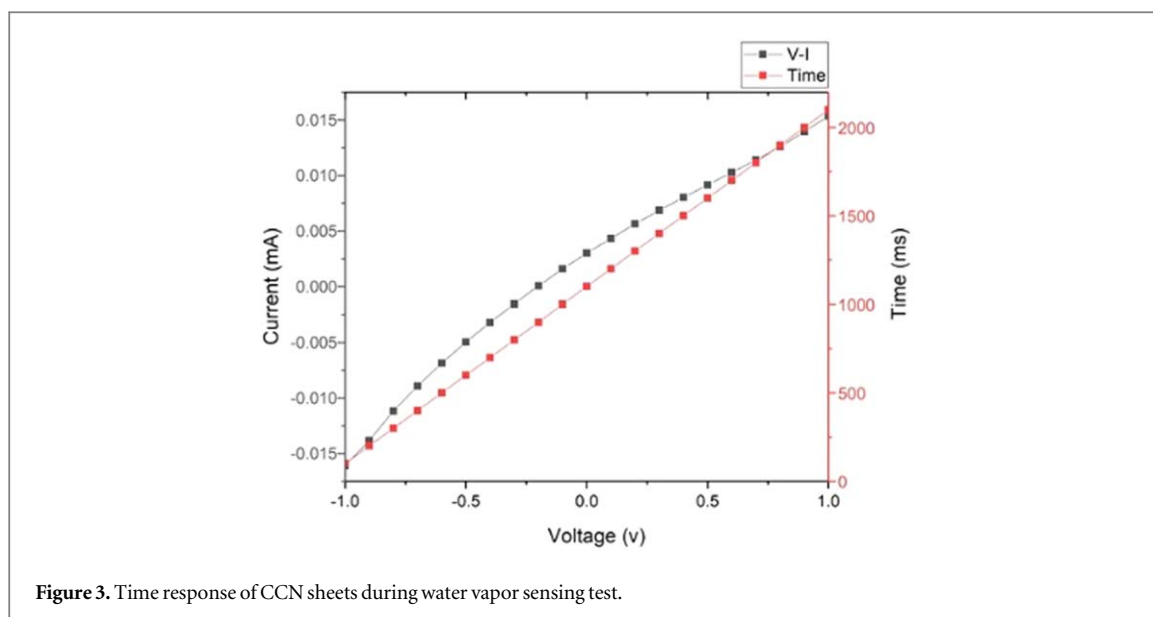


**Figure 3.** Time response of CCN sheets during water vapor sensing test.

**Table 1.** The resistance of CCN sheets at different loading of CNH percent of water vapor.

Sample	Resistance $k\Omega$
5 wt%	Nil
10 wt%	Nil
25 wt%	162
50 wt%	53

**Table 2.** Resistance of CCN sheet for different water vapor% (RH%).

Water vapor (RH%)	Resistance $k\Omega$
Dry	53
25	62.14
50	71.24
75	85.7
90	103.6

Water vapor sensing of CCN sheets is possible due to the water accepting property of cellulose, and a minimum doping concentration of 25 wt% is required for conductivity to occur in the CCN composite sheets. Hence the resistance of a thin film (of 50 wt%) CCN sheet when exposed to different levels of water vapor detection was recorded, see table 2. The water sensing property is measured by coating the freestanding CCN sheet with electrically conductive silver paint on either end to obtain ideal ohmic contact with the probes. The CCN sheet was placed in a chamber with probes attached to either end of the CCN sheet. Water vapor is fed into the chamber through the inlet valve and a digital hygrometer is setup inside the chamber to measure the relative humidity (RH%) [19]. The resistance of the CCN sheets was measured at different levels of RH%. During the exposure to water vapor, a change in the resistance was observed in the CCN sheets, due to the presence of the cellulose interfaces between the CNH aggregates that affected the resistance path. The resistance values for different RH% are shown in table 2. Comparing the resistance of CCN sheets before and after the exposure to water vapor, the resistance has gradually increased with the increase in the water vapor %. The dynamic change in resistance can also be seen by the change in resistance versus time, as shown in figure 3 measured by time, of exposure. The graph shows time (ms) versus Resistance, which is a curved path showing the difference between dry response as in figure 7 and wet response in figure 3. Hydroxyethylcellulose has long branches of polymeric chains with -OH groups that accept water molecules and hence possesses the hygroscopic property. An illustration of the vapor sensing setup is shown in figure 8.

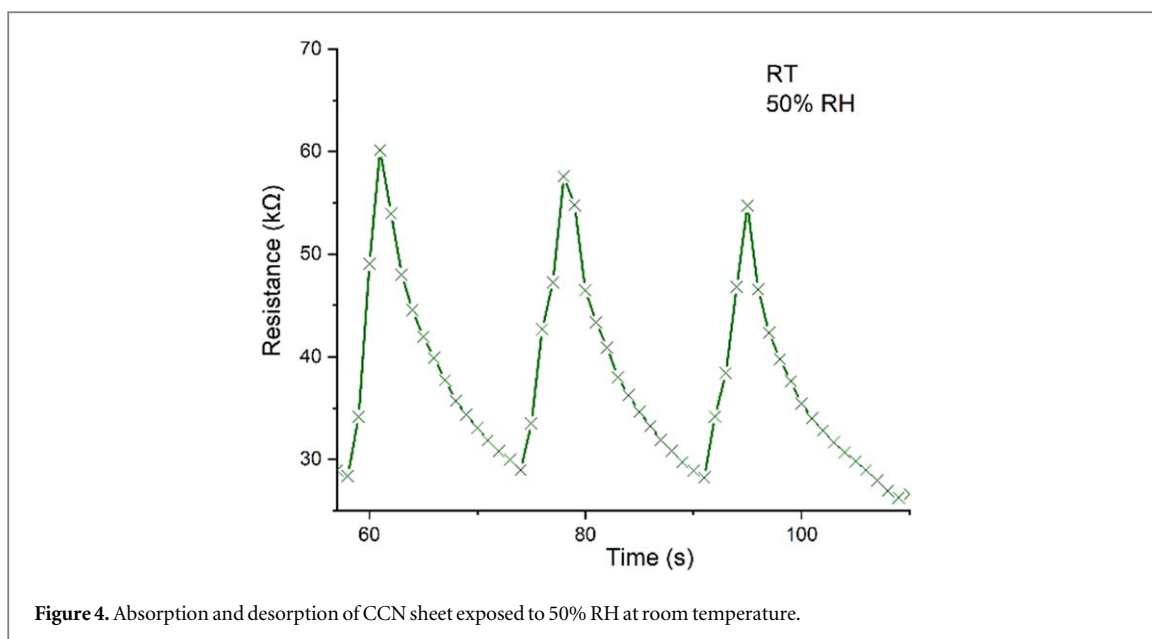


Figure 4. Absorption and desorption of CCN sheet exposed to 50% RH at room temperature.

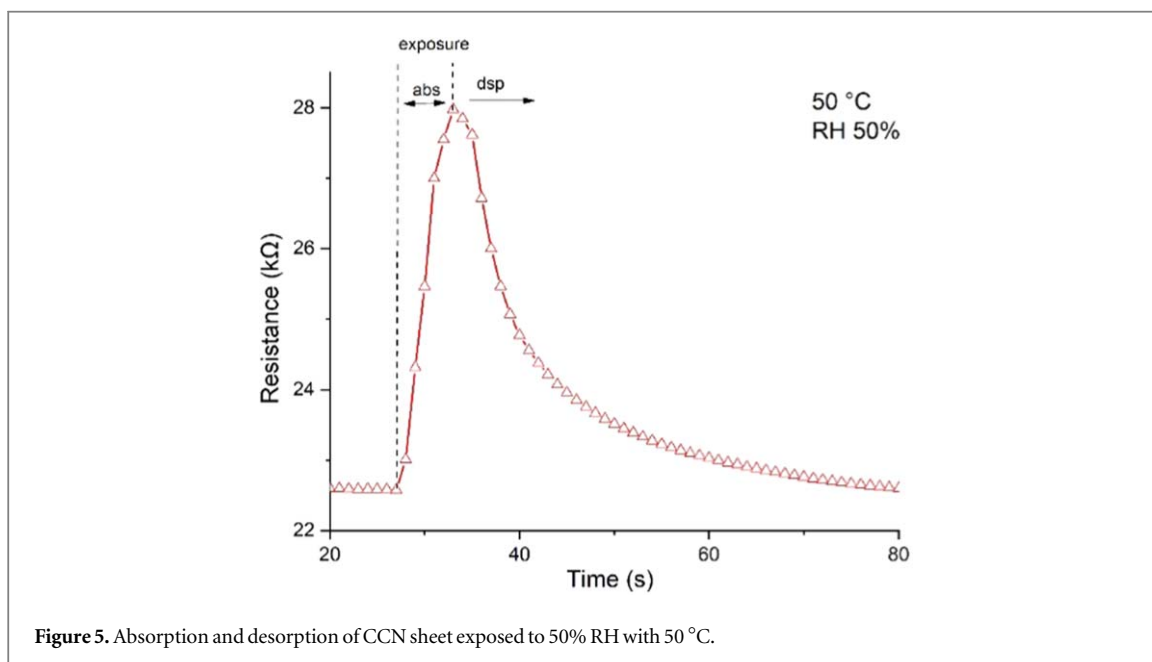
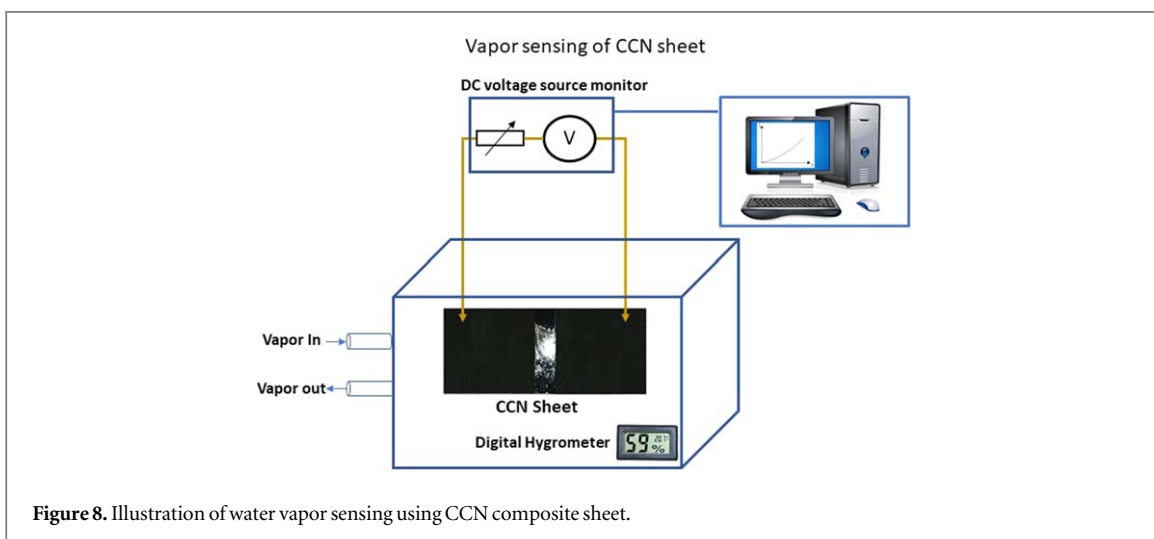
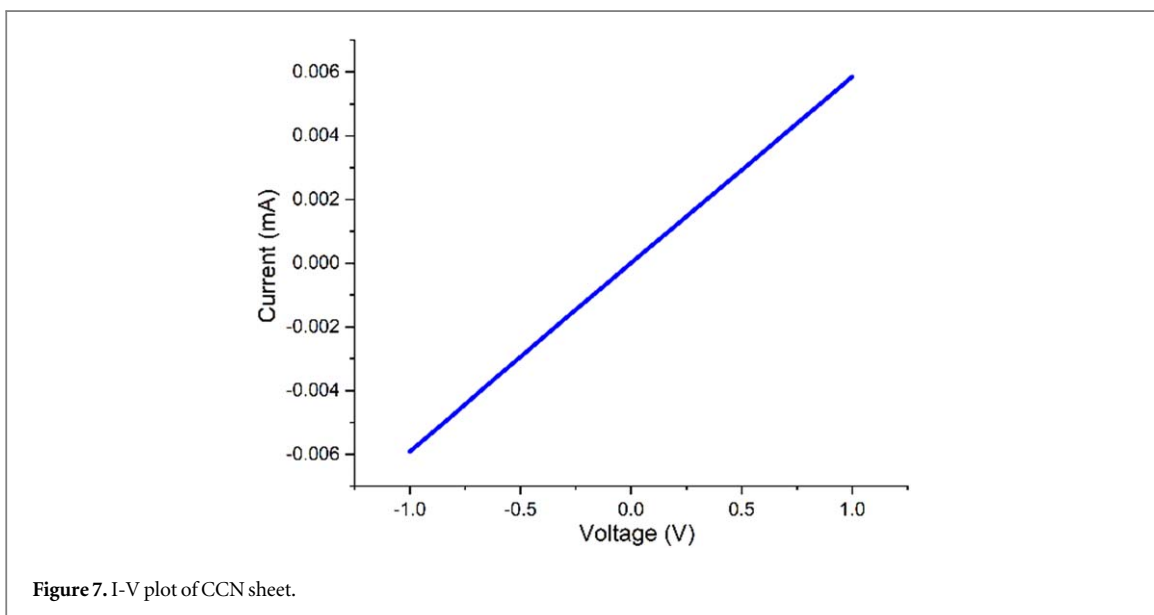
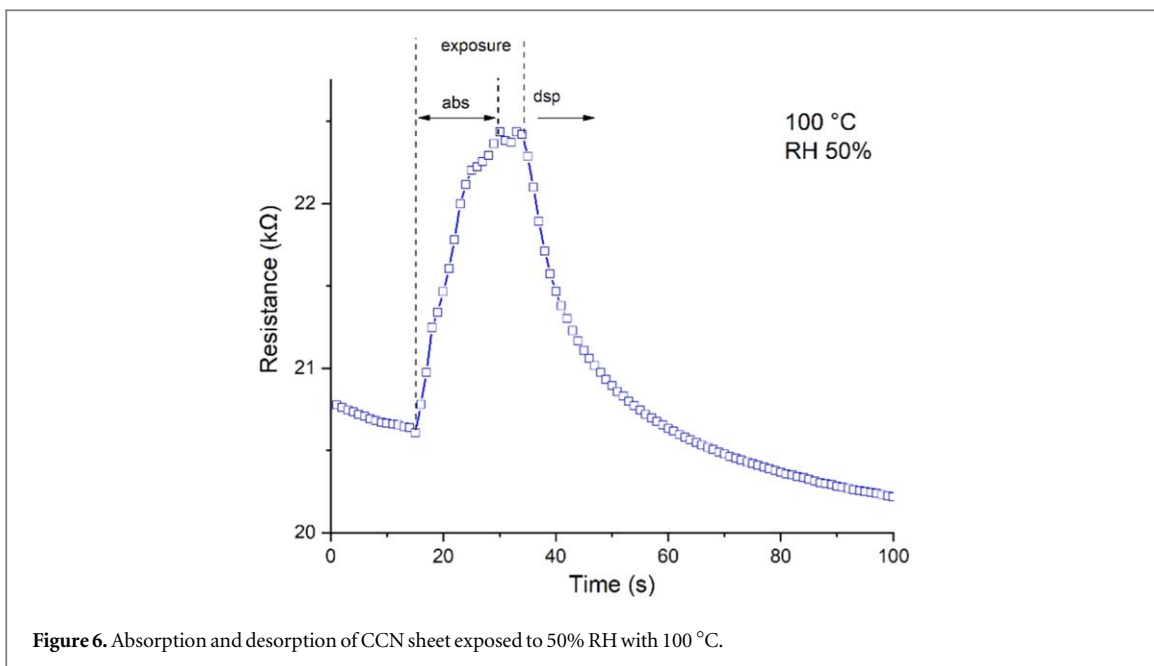


Figure 5. Absorption and desorption of CCN sheet exposed to 50% RH with 50 °C.

To calculate the rate of desorption of the water vapor on the CCN sheets, at room temperature, 50 °C, 100 °C at 50% RH, was applied with a constant voltage to measure the rate of change in the resistance versus time. Initially at room temperature the response time of the CCN sheet to water vapor was 4 s, and the recovery time was at 13 s at 50% RH as shown in figure 4. Similarly at 50 °C, the absorption of water vapor was very high as the resistance of the CCN sheet increased from 22.5 kΩ to 27.9 kΩ in 4 s to reach maximum peak absorption. After the exposure of water vapor, the recovery time for the CCN sheet maximum resistance of 100% to 10% was 13 s, as shown in the figure 5. Similarly, when the CCN sheet was heated at 100 °C, and exposed to 50% RH, the resistance increased from 20.6 kΩ to 22.4 kΩ in 13 s. After the exposure of water vapor, the resistance decreased exponentially and the recovery time from 100% to 10% resistance drop was 18 s as shown in figure 6. It is observed that at 50 °C the increase in the resistance was twice higher than heating at 100 °C, this is because the absorption at lower temperatures on the CCN sheet is higher than the desorption.

Scanning electron microscopy (SEM) was used to explore the surface morphology of the CCN composite sheets. A small piece of the CCN sheet was cut and placed on-to the sample holder, and the accelerating voltage was 5 kV. Figure 9(a) shows that, at minimum doping concentration of 5 wt%, the surface of the CCN sheets has a visibly smooth surface when observed at  $\times 700$  magnification. Comparatively, for CCN composite sheets at a loading concentration of 10 wt%, rough surfaces are observed at  $\times 1000$  magnification, indicating the surface



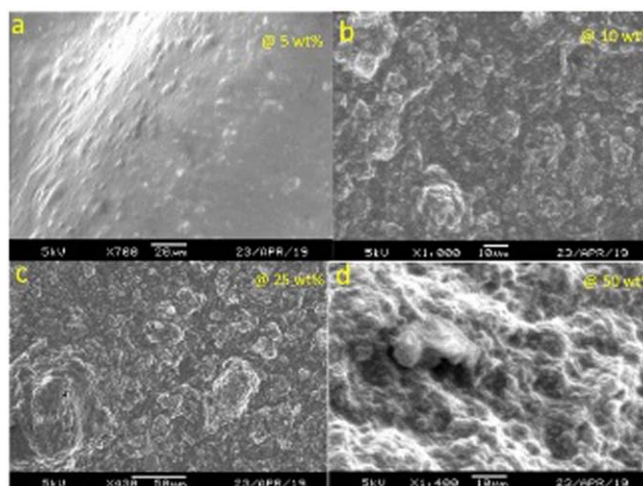


Figure 9. SEM of CCN sheets at different loading concentrations.

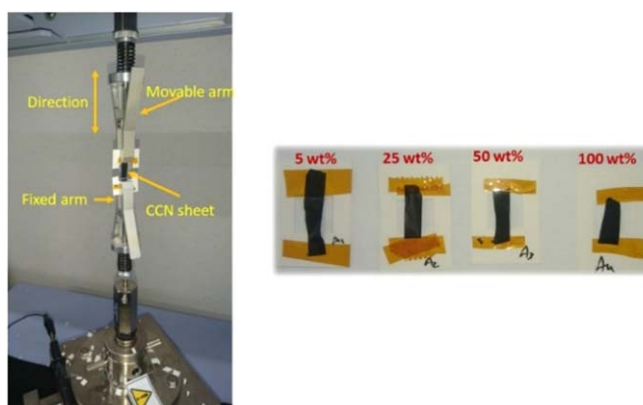
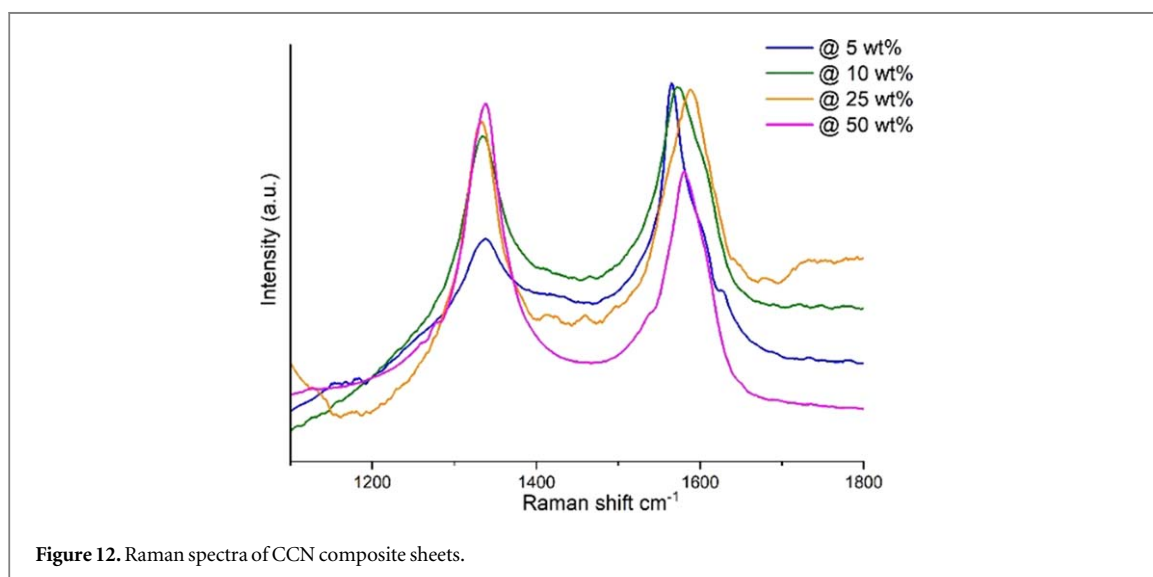
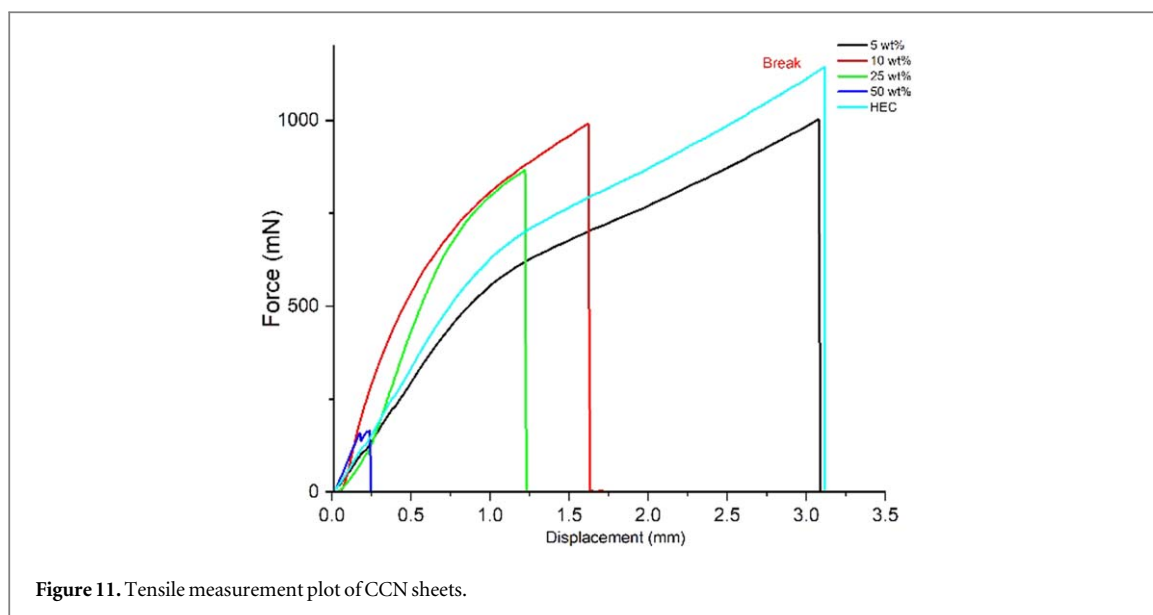


Figure 10. Samples for tensile strength measurement.

morphology has changed for the doubled loading concentration, as seen in figure 9(b). This can also be seen with a 25 wt% loading concentration of CNHs observed at  $\times 430$  magnification, which also has a similar morphology to that of 10 wt% or 50 wt%, as in figure 9(c). Also, at a 50 wt% loading concentration of CNH, the surface morphology is seen to be rough when observed at  $\times 1400$  magnification, as in figure 9(d). The surface roughness increases as the concentration of CNH loading increases. An irregular or rough surface of the CCN composite sheets increases the surface area, and thus improves the interaction between the CCN surface and the water vapor molecules, which is similar to the cellulose and CNT aerogel synthesized by Haisong *et al* [19]. It also aids in rapid re-evaporation of the absorbed water vapor molecules, hence retaining the original resistance value of the CCN sheet. The surface roughness increases with an increase in the loading concentration of CNHs. The tensile strength measurements and the surface morphology lead to the conclusion that the maximum loading concentration of CNHs possible is 50 wt%. This helps in understanding that for any further increase in the loading concentration of CNHs, the morphology leads to cracks, which affect the geometry of the CCN sheets. For the application of electromagnetic shielding, porous structures have reported before [20], but thin films are not yet been explored.

The samples for tensile strength measurement were prepared by carefully cutting 20 mm x 10 mm sample sheets and placing them in the paper holder fastened with glue tape. The active area under tensile measurement is 10 mm x 10 mm. The paper holders were placed in the clip arms of the tensile measurement instrument and the tension initially adjusted to a few milli-newtons to hold the thin film sheets in place, as shown in figure 10. When force is applied to the CCN sheets, the displacement is not linear for 5 wt%, 10 wt%, and 25 wt%. This indicates that the CCN composite thin films have a perceptible amount of elastic property. Also, the displacement of the CCN sheets is inversely proportional to the loading concentration of the CNH. Figure 11 shows that as the loading concentration increases, the displacement of the CCN composite sheets decreases. For





5 wt% loading concentration of CCN composite sheets, the displacement or maximum stretchability was 3.08 mm at 1002.63 mN. Whereas for 10 wt% loading concentration of CNH, the displacement is reduced to 1.62 mm at 990.73 mN. This means that doubling the loading concentration of the CNH only reduced the strength of the sheets by 1%, whereas the stretchability was affected by approximately 55%.

Similarly, for loading concentration of 25 wt% has a displacement of 1.22 mm at 865.6 mN, which implies the effect of loading has reduced the displacement by 20% and the strength by 15% w.r.t the previous loading concentration. Lastly, at 50 wt% loading concentration, the displacement was measured to be about 0.24 mm at 23 mN, implying that the thin film sheets cannot sustain any further increase in the loading concentration, and even a slight force applied would lead to breaking. This sensitivity of the CCN composite sheets indicates that the maximum loading to obtain a conductive thin film sheet of 100  $\mu\text{m}$  thickness is 50 wt%.

Raman spectroscopy determines the purity of the bonds and defects and evaluates the presence of CNHs on other related carbons in the sheets. For CNHs, two significant peaks are observed at  $1585\text{ cm}^{-1}$  and  $1340\text{ cm}^{-1}$  that correspond to the graphitic and disorder structures, i.e., the G and D bands [21] depicted in figure 12. As the presence of CNH in all the doping concentrations increases, the intensity is found to increase. At 5 wt% loading of CNHs, the D band is quite low compared to the other higher loading concentration.

Fourier transform infrared spectroscopy (FT-IR), one of the most efficient and non-destructive methods of performing functional group analysis, used to evaluate the interaction of CNH and cellulose. Because cellulose is a hygroscopic material, whereas CNH is slightly dispersible in distilled water, OH– bonds were found in a deep

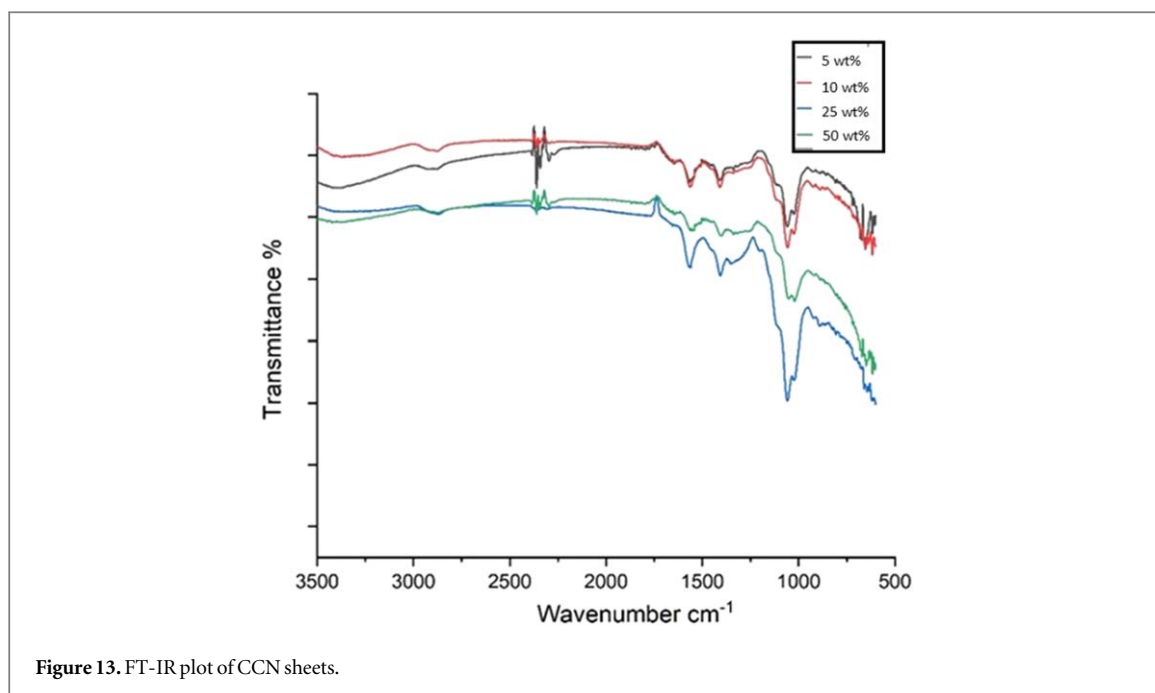


Figure 13. FT-IR plot of CCN sheets.

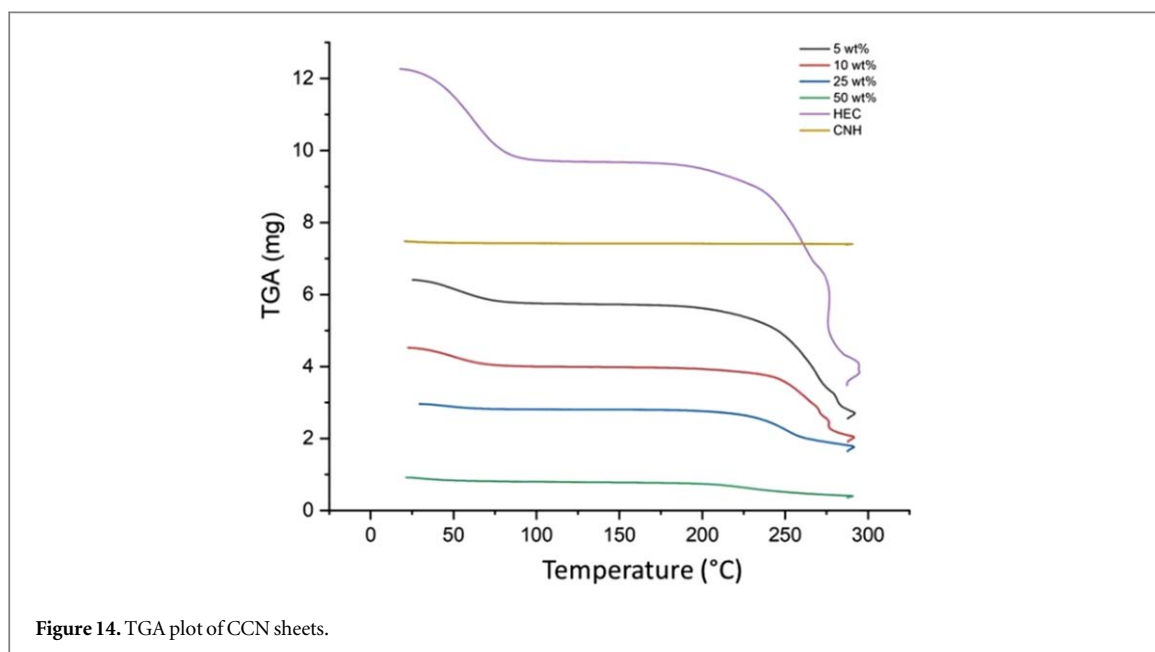


Figure 14. TGA plot of CCN sheets.

stretching around  $3340\text{ cm}^{-1}$  and a weak absorption at  $2896\text{ cm}^{-1}$ . This also explains that the stretching and flexible nature is due to the mediation of OH<sup>-</sup> molecules binding between CNH and cellulose [22], as shown in figure 13.

Furthermore, the OH<sup>-</sup> bond allows retaining the geometry of sheets with a thickness of  $<50\ \mu\text{m}$ . Hydroxyethylcellulose has a very intense characteristic absorption band at  $1065\text{ cm}^{-1}$ , which is assigned to the stretching vibrations of the <sup>-</sup>(COH) functional group [23]. A significant absorption band is observed at  $1562\text{ cm}^{-1}$  in all the samples, reflecting the asymmetric stretching vibrations of COO groups.

The thermal stability of various CCN composites is plotted in figure 14 and table 3. The differential thermogravimetric analysis shown in figure 15 suggests that all the composites display single step decomposition profiles. The thermal stability data suggests that after the addition of CNHs, the thermal stability of the composite film is significantly increased due to the organic inorganic hybrid nature of the mixture and the high thermal stability of the loaded CNHs material. Generally, the onset decomposition temperature of the cellulose film is around  $50\text{ }^{\circ}\text{C}$ – $100\text{ }^{\circ}\text{C}$  [24], whereas, after loading carbon nanohorns, the thermal stability is increased to around  $250\text{ }^{\circ}\text{C}$ . However, there is an abnormality in the thermal stability for 10 wt% loading, which shows a higher thermal stability than the remaining loadings, that may be due to the uniform dispersion of CNH in the

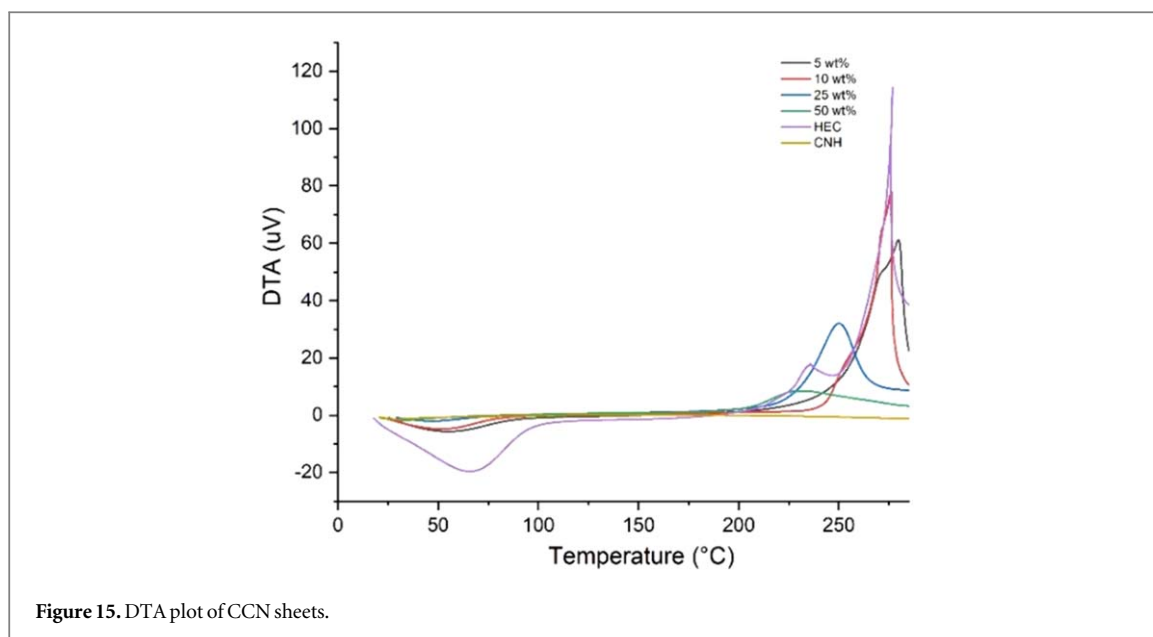


Figure 15. DTA plot of CCN sheets.

Table 3. TGA details of onset decomposition  $T_{onset}$  and Max decomposition  $T_{max}$ .

CNH (mg)	HEC (mg)	CNH %	Onset decomposition $T_{onset}$	Max decomposition $T_{max}$
10	200	4.8	240	275
20	200	9.1	180	230
50	200	20.0	220	250
100	200	33.3	240	275

composite. With the increase of loading from 4.8% to 9.1%, the thermal stability is considerably reduced, which may be due to the formation of an agglomeration of the loaded CNH.

However, the further addition of CNH (20 and 33.3%) improved the thermal stability of the film, which may be due to the dominating behaviour of the high mechanical strength of the loaded CNH material.

#### 4. Conclusion

This work provides a simple, efficient, and effortless method for the synthesis of cellulose–carbon nanohorn composite sheets with different loading concentrations. The loading concentration ratios shed light on understanding the maximum loading concentration possible to draw a freestanding thin film sheet using the CCN composite. The tensile strength measurements revealed the strength of the sheets and helped to understand the loading concentration versus the strength of the CCN sheets. The change in resistance of the CCN sheets in response to water vapor leads to the conclusion that the CCN composite material has the potential for sensing applications, and additional research to explore further is encouraged. It is observed that, in order to achieve high flexibility, the loading concentration of CNHs should be minimum, as high loading concentrations affect flexibility and strength.

#### Acknowledgments

The authors thank Dr V Swapna for her kind help in analyzing the TGA data. The authors also thank SGU-MEXT for its financial support for International students to pursue a PhD in Japan.

## ORCID iDs

Karthik Paneer Selvam  <https://orcid.org/0000-0003-1927-6755>

Hirota Inoue  <https://orcid.org/0000-0002-3881-497X>

Yasuhiko Hayashi  <https://orcid.org/0000-0002-4113-5548>

## References

- [1] Du X, Zhang Z, Liu W and Deng Y 2017 Nanocellulose-based conductive materials and their emerging applications in energy devices - A review *Nano Energy*. **35** 299–320
- [2] Zhao D et al 2017 Study of co-solvent effect on the dissolution of cellulose in ionic liquid and the properties of regenerated cellulose fibres *21st International Conference on Composite Materials* **12** 937–42
- [3] Jackson J K, Letchford K, Wasserman B Z, Ye L, Hamad W Y and Burt H M 2011 The use of nanocrystalline cellulose for the binding and controlled release of drugs *Int. J. Nanomed.* **6** 321–30
- [4] Zhang T et al 2010 Biotemplated synthesis of gold nanoparticle-bacteria cellulose nanofiber nanocomposites and their application in biosensing *Adv. Funct. Mater.* **20** 1152–60
- [5] Wang S et al 2016 Reinforcement of lignin-based carbon fibers with functionalized carbon nanotubes *Compos. Sci. Technol.* **18** 116–22
- [6] Swatloski R P, Spear S K, Holbrey J D and Rogers R D 2002 Dissolution of cellulose with ionic liquids *J. Am. Chem. Soc.* **124** 4974–5
- [7] Zhang M, Yamaguchi T, Iijima S and Yudasaka M 2009 Individual single-wall carbon nanohorns separated from aggregates *J. Phys. Chem. C* **2009** **113** 11184–6
- [8] Fan L, Li B, Zhang N and Sun K 2015 Carbon nanohorns carried iron fluoride nanocomposite with ultrahigh rate lithium ion storage properties *Sci. Rep.* **5** 12154
- [9] Xu J, Tomimoto H and Nakayama T 2011 What is inside carbon nanohorn aggregates ? *Carbon* **49** 2074–8
- [10] Mercatelli L, Sani E, Giannini A, Di Ninni P, Martelli F and Zaccanti G 2012 Carbon nanohorn-based nanofluids: characterization of the spectral scattering albedo *Nanoscale Res. Lett.* **7** 96
- [11] Rastogi R, Kaushal R, Tripathi S K, Sharma A L, Kaur I and Bharadwaj L M 2008 Comparative study of carbon nanotube dispersion using surfactants *J. Colloid Interface Sci.* **328** 421–8
- [12] Camilli L and Passacantando M 2018 Advances on sensors based on carbon nanotubes *Chemosensors* **6** 1–17
- [13] Kong J et al 2000 Nanotube molecular wires as chemical sensors *Science* **287** 622–5
- [14] Shimizu Y and Egashira M 1999 Basic aspects and challenges of semiconductor gas sensors *MRS Bull.* **24** 18–24
- [15] Penza M, Rossi R, Alvisi M and Serra E 2010 Metal-modified and vertically aligned carbon nanotube sensors array for landfill gas monitoring applications *Nanotechnology* **21** 105501
- [16] Cao C L, Hu C G, Fang L, Wang S X, Tian Y S and Pan C Y 2011 Humidity sensor based on multi-walled carbon nanotube thin films *J. Nanomater.* **2011**
- [17] Arunachalam S, Izquierdo R and Nabki F 2019 Low-hysteresis and fast response time humidity sensors using suspended functionalized carbon nanotubes *Sensors* **19**
- [18] Park D H, Kan T G, Lee Y K and Kim W N 2013 Effect of multi-walled carbon nanotube dispersion on the electrical and rheological properties of poly(propylene carbonate)/poly(lactic acid)/multi-walled carbon nanotube composites *J. Mater. Sci.* **48** 481–8
- [19] Qi H, Liu J, Pionteck J, Pötschke P and Mäder E 2015 Carbon nanotube-cellulose composite aerogels for vapour sensing *Sensors Actuators, B Chem.* **213** 20–6
- [20] Huang H D et al 2015 Cellulose composite aerogel for highly efficient electromagnetic interference shielding *J. Mater. Chem. A*. **3** 4983–91
- [21] Lin Z et al 2017 Surface modification of carbon nanohorns by helium plasma and ozone treatments *Jpn. J. Appl. Phys.* **56** 01AB08
- [22] Orhan B, Ziba C A, Morcali M H and Dolaz M 2018 Synthesis of hydroxyethyl cellulose from industrial waste using microwave irradiation *Sustain Environ. Res.* **28** 403–11
- [23] Mukerabigwi J F et al 2016 Eco-friendly nano-hybrid superabsorbent composite from hydroxyethyl cellulose and diatomite
- [24] Shen W, Hu T and Fan W 2014 Cellulose generated-microporous carbon nanosheets with nitrogen doping *RSC Adv.* **4** 9126–32